

ORIGINAL ARTICLE

Changes in the Proliferative Program Limit Astrocyte Homeostasis in the Aged Post-Traumatic Murine Cerebral Cortex

Gábor Heimann¹, Luisa L. Canhos^{1,2,3}, Jesica Frik^{1,2,4}, Gabriele Jäger¹, Tjasa Lepko^{2,3}, Jovica Ninkovic^{1,2,3}, Magdalena Götz^{1,2,5} and Swetlana Sirko^{1,2}

¹Physiological Genomics, Biomedical Center, Ludwig-Maximilians-University Munich, 82152 Planegg, Germany, ²Institute of Stem Cell Research, Helmholtz Center Munich, German Research Center for Environmental Health (GmbH), 85764 Neuherberg, Germany, ³Graduate School of Systemic Neurosciences, Ludwig-Maximilians-University Munich, 82152 Planegg, Germany, ⁴Institute of Biotechnology and Molecular Biology (IBBM), Department of Biological Sciences, 1900 La Plata, Argentina and ⁵Synergy, Excellence Cluster of Systems Neurology, Biomedical Center, Ludwig-Maximilians-University Munich, 82152 Planegg, Germany

Address correspondence to Swetlana Sirko, Physiological Genomics, Biomedical Center, Ludwig-Maximilians-University Munich, Großhadener Str. 9, 82152 Planegg, Germany. Email: swetlana.sirko@med.uni-muenchen.de

Abstract

Aging leads to adverse outcomes after traumatic brain injury. The mechanisms underlying these defects, however, are not yet clear. In this study, we found that astrocytes in the aged post-traumatic cerebral cortex develop a significantly reduced proliferative response, resulting in reduced astrocyte numbers in the penumbra. Moreover, experiments of reactive astrocytes *in vitro* reveal that their diminished proliferation is due to an age-related switch in the division mode with reduced cell-cycle re-entry rather than changes in cell-cycle length. Notably, reactive astrocytes *in vivo* and *in vitro* become refractory to stimuli increasing their proliferation during aging, such as Sonic hedgehog signaling. These data demonstrate for the first time that age-dependent, most likely intrinsic changes in the proliferative program of reactive astrocytes result in their severely hampered proliferative response to traumatic injury thereby affecting astrocyte homeostasis.

Key words: aging, brain injury, cell division, GFAP, glia, reactive gliosis, self-renewal, Shh

Introduction

Aging is associated with a plethora of morphological, ultrastructural and epigenetic modifications, which can significantly impair brain functioning (Lynch et al. 2010; Chisholm et al. 2015). It is thus not surprising that the cellular reactions to pathological processes in the brain differ profoundly between young

and older organisms (Buga et al. 2008; Juraska and Lowry 2012). Indeed, adverse recovery and poor outcome following traumatic injury or ischemic episode in aged patients and experimental animals provide compelling evidence that the young brain is able to recover much better than the old one (Copen et al. 2001; Badan et al. 2003; Zhang et al. 2005; Fonarow et al. 2010;

Gargano et al. 2011; Pekna et al. 2012). Since the acute phase events are of greatest importance for functional outcomes after invasive brain injury (Alexander 1994; Moppett 2007; Dostovic et al. 2009), the pronounced regenerative capacity within the young brain parenchyma over the first few days after a pathological event may underlie better recovery from damage. It is important to note that this short time span after damage is characterized by various reactions of neurons and glial cells, including astrocytes (Sirko et al. 2013; Burda and Sofroniew 2014). Due to the multiple roles that reactive astrocytes, and especially their proliferating subset have (Burda and Sofroniew 2014; Verkhratsky et al. 2014a, 2014b; Anderson et al. 2016), transcriptional mechanisms regulating their injury-induced response have been the focus of recent studies in postnatal or young adult animals (Zamanian et al. 2012; Sirko et al. 2015). However, still relatively little is known about age-dependent properties of astrocytes in the post-traumatic brain (see in review Verkhratsky et al. 2016).

As physiological aging is associated with morphological and molecular changes in astrocytes (Unger 1998; Lynch et al. 2010; Middeldorp and Hol 2011; Orre et al. 2014), the region-specific effects of aging on reactive astrocytes may potentially interfere with restorative process within the injured parenchyma, and consequently, limit the recovery of aged animals after lesion. Especially, in the post-traumatic cerebral cortex gray matter (GM), astrocytes have the potential to exert powerful and long-term influences on regenerative processes through their injury-induced proliferation, as in this brain region astrocytes do not migrate toward the injury site, and recruitment of astroglial population after injury relies solely on proliferation in a specific niche (Bardehle et al. 2013). In spite of this, the effect of aging on astrocyte proliferation and restoration of the astroglial equilibrium in the injured GM is still unclear.

We, therefore, examined here the changes in proliferative astrocyte response in the somatosensory GM of young, middle-aged and old mice throughout the first week post-injury. The results of our study shed new light on how the aging process changes the proliferative program of reactive astrocytes, thereby impairing the recovery of astrocyte numbers in the injured GM parenchyma.

Materials and Methods

Animals

Experiments were performed with C57BL/6J mice (Charles River Laboratories), Tg(Aldh111-eGFP)OFC789Gsat mice (Heintz 2004), TgN(hGFAP-EGFP)GFEA mice (Nolte et al. 2001), and double transgenic mice crossbred from TgN(GFAP-mRFP1) mice (Hirrlinger et al. 2005) and B6.Cg-Tg(Fucci)504Bsi(RBRC02706) (Fucci-S/G2/M-Green:mAG-hGeminin [1/110]) mice, expressing the S/G2/M phase-specific fusion-protein mAG-hGeminin (Sakaue-Sawano et al. 2008) (RIKEN BioResource Center). Animals were allocated to experimental groups regarding their genotype and kept under standard conditions with access to water and food ad libitum. Animal handling and experimental procedures were performed in accordance with German and European Union guidelines and were approved by the State of Upper Bavaria. All efforts were made to minimize suffering and number of animals used.

Surgical Procedures

Stab wound injury was performed in the somatosensory cortex, as previously described (Buffo et al. 2008; Heinrich et al. 2014).

Briefly, animals were anesthetized and received a 1.2 mm stab wound into the cortical GM parenchyma with a lancet-shaped knife (Alcon) along the anteroposterior axis at the following coordinates from bregma: anteroposterior -0.8 to -2.0 , mediolateral 1.6 – 2.0 mm, and dorsoventral -0.6 . For the in vivo treatment with Smoothened agonist (SAG; Calbiochem) (Frank-Kamenetsky et al. 2002), SAG (0.15 mg in 0.5% methylcellulose/0.2% Tween80 per 10 g body weight) was administered orally once a day for 5 days, starting 2 h after stab wound injury (Sirko et al. 2013). All experimental procedures were performed in accordance with the animal welfare policies of, and approved by the State of Bavaria.

Immunohistochemistry

After transcardial perfusion with phosphate-buffered saline (PBS) and then 4% paraformaldehyde (PFA) in PBS, brains were postfixed in 4% PFA for 4 h at 4°C , and then cryoprotected in 30% sucrose in PBS. Sections of $40\mu\text{m}$ thickness were processed for immunohistochemistry, as previously described (Simon et al. 2011). The following primary antibodies were used: anti-glial fibrillary acidic protein (GFAP) (mouse, 1:400; Sigma-Aldrich) or anti-GFAP (rabbit, 1:500; Dako), anti-BrdU (rat, 1:200; Biozol), anti-Ki-67 (rabbit, 1:100; Life Technologies), anti-s100 β (mouse, 1:250; Sigma-Aldrich), anti-aldehyde dehydrogenase 1 family member L1 (Aldh111) (mouse, 1:200; Millipore), anti-Iba1 (rabbit, 1:500; Wako), and anti-NG2 (rabbit, 1:200; Chemicon). To detect the various primary antibodies, we used subclass specific secondary antibodies coupled with Alexa488 (1:500), Alexa594 (1:1000), Alexa633 (1:1000), Cy3 (1:500), or Cy5 (1:1000) (all from Dianova). All antibodies were diluted in PBS-TritonX with 10% normal goat serum. Proliferating cells were labeled with 5'-bromo-deoxyuridine (BrdU; Sigma-Aldrich) added to the drinking water (1 mg/mL water containing 1% sucrose) for 5 consecutive days. BrdU incorporation was monitored in free-floating sections pretreated with 0.01 M sodium citrate (pH6) at 95°C for 24 min, as previously described (Simon et al. 2011).

Adherent Culture and Immunocytochemistry

For the adherent culture, cortical cells of the post-traumatic somatosensory GM were dissociated with activated papain (30 U/mL) from punched tissue samples covering an area of 1.25 mm radius from the lesion site at 5 days post-injury (dpi). After 15 min at 37°C , dissociation was stopped with ovomucoid (1 mg/mL trypsin inhibitor (Sigma), 50 $\mu\text{g}/\text{mL}$ bovine serum albumin (Sigma), 40 $\mu\text{g}/\text{mL}$ DNaseI (Worthington), in L-15 medium (Sigma)), and the suspension was then centrifuged for 5 min at 200g. Cells were resuspended in culture medium containing Dulbecco's Modified Eagle medium: nutrient mixture F-12 (DMEM/F-12), 10% fetal calf serum, 1% B27 Supplement, 2 mM L-Glutamine, 1% penicillin-streptomycin, FGF-2 and EGF both at 20 ng/mL (all from Invitrogen) and 200,000 cells were plated in 2 mL medium per well in 24-wells cell culture plates coated with poly-L-ornithine (100 $\mu\text{g}/\text{mL}$) and laminin (20 $\mu\text{g}/\text{mL}$). To adapt to culture conditions, cells were kept for 2 days without medium change. After 2 days in vitro (div), debris was washed off with PBS, and 2 mL of freshly prepared medium with or without SAG (0.5 mM, Calbiochem) was added to cell cultures. The cell culture plates were then transferred to the incubator of the time-lapse microscope for continuous imaging for 7 days.

The number of surviving cells within individual cultures was determined by using data recorded in the individual wells at the beginning of time-lapse imaging (time point 0).

The average cell density was calculated per mm^2 for each experimental group. Although there were some variations in the number of adherent cells between age-groups (166 ± 20 , 147 ± 23 , and 130 ± 25 cells/ mm^2 in the cultures prepared from the injured GM of 2-, 6-, and 12-month-old animals, respectively, $n = 6$), these differences were not significant ($P = 0.290$, $P = 0.289$, $P = 0.330$, 2 month vs. 6 month, 2 month vs. 12 month, 6 month vs. 12 month, respectively). The growth profile was determined by analyses of cell numbers in the same cell cultures at the start and end point (168 h) of imaging. The average expansion rate among all cell cultures was 6.7 ± 0.8 (6.4 ± 0.8 , 5.9 ± 0.6 , and 7.9 ± 0.8 in the cultures prepared from the injured GM of 2-, 6-, and 12-month-old animals, respectively; $n = 6$) with no significant differences between experimental groups ($P = 0.596$, $P = 0.102$, $P = 0.067$, 2 month vs. 6 month, 2 month vs. 12 month, 6 month vs. 12 month, respectively), indicating that the cultured reactive glia from young, middle-age, or old animals may grow in a similar manner. The identity of the adherent cells at the start point of live cell imaging was determined in cultures prepared in parallel, which were fixed and immunostained for GFAP (rabbit, 1:300; Dako), Iba1 (rabbit, 1:300; Wako), NG2 (rabbit, 1:200; Chemicon), O4 (mouse, 1:50; Millipore), NeuN (mouse, 1:250; Millipore), and β III-tubulin (mouse, 1:250; Promega), as previously described (Sirko et al. 2009).

After time-lapse imaging, cells were fixed and stained for GFAP (rabbit, 1:300; Dako), β III-tubulin (mouse, 1:250; Promega), and O4 (mouse, 1:50; Millipore), as described previously (Sirko et al. 2015). Nuclei were visualized with 4',6'-diamidino-2-phenylindole (DAPI) (0.1 mg/mL; Sigma-Aldrich). After immunostaining, cells were imaged at the corresponding locations with the time-lapse microscope. For the control experiments, we used cell cultures prepared from the intact GM, as well as reactive gliosis cells cultured in the cyclopamine-containing medium (5 nM, Sigma-Aldrich).

Time-Lapse Video Microscopy

Time-lapse video microscopy and single-cell tracking of primary cortical cultures were carried out with a cell observer (Zeiss) in an incubator with a constant temperature of 37°C and 5% CO_2 . Phase-contrast images were acquired every 5 min using a phase-contrast microscopy objective (Zeiss), fluorescence images every 450 min with an AxioCamHRm camera and Zeiss AxioVision 4.7 software. Single-cell tracking was carried out using a self-written computer program (Rieger et al. 2009; Hilsenbeck et al. 2016). Videos were assembled using ImageJ 10.2 software (National Institutes of Health).

Neurosphere Culture

Neurosphere cultures were prepared from the cells of the injured somatosensory GM tissue that was punched from areas spanning 1.25 mm in radius from the lesion site at 5 dpi. Samples were digested with Trypsin (0.025%) for 20 min at 37°C and digestion was stopped with the ovomucoid-containing solution described above. Cells were centrifuged at 1500 r.p.m. for 5 min, resuspended in neurosphere medium containing DMEM/F-12, 1% B27 Supplement, 2 mM L-Glutamine, 1% penicillin-streptomycin, FGF-2, and EGF both at 20 ng/mL (all from Invitrogen) and plated in 24-wells cell culture plates at a density of 5 cells/ μL . For some experiments, we used 0.5 mM SAG (Calbiochem), which was added at the beginning of the experiment only. The number and size of generated neurospheres was

determined after 7 or 14 div, and individual neurospheres were assessed for self-renewal as described earlier (Sirko et al. 2015).

Purification of cells using Fluorescence-Activated Cell Sorting

Single-cell suspensions were prepared from the somatosensory GM tissue of either intact mice (2 animals per age-group in distinct biological samples) or injured mice (3 animals per age-group in pooled biological samples) using the same procedure as described above. Following dissociation, cells were resuspended in medium containing DMEM/F-12, 1% B27 Supplement, 2 mM L-Glutamine, 1% penicillin-streptomycin (all from Invitrogen), and filtered with a 40 μm strainer. Cell viability was determined via staining with propidium iodide (1:1000, Sigma) in parallel samples processed from C57Bl/6 mice. GFAP-mRFP+, GFAP-GFP+, and Aldh111-eGFP+ cells were isolated by fluorescence-activated cell sorting (FACSaria, BD). Gating parameters were set by side and forward scatter to eliminate debris and aggregated cells. Cells were sorted into RNase-free eppendorfs containing RLT buffer with 1% β -mercaptoethanol and further processed for qPCR analysis.

RNA Extraction and Quantitative RT-PCR

RNA from FACS-sorted cells was extracted with the RNeasy Plus Micro Kit (Qiagen) according to manufacturer's instructions, and genomic DNA was removed. RNA was retrotranscribed with SuperScriptIII Reverse Transcriptase and Random Primers (Roche). Real-time qPCR was performed on LightCycler480 (Roche) with the LightCycler Probe Master kit (Roche) and Monocolor Hydrolysis Probe (Roche) according to manufacturer's instructions. The expression of each gene was analyzed in 3 technical replicates per biological sample, whereas each biological sample of the Aldh111-GFP+ astrocytes was composed of a pool of cells sorted from the injured GM tissue from 3 animals per age-group. Data were processed with the $\Delta\Delta\text{Ct}$ method (Livak and Schmittgen 2001) and the levels of gene transcripts were normalized to that of the hypoxanthine-guanine phosphoribosyltransferase transcript. Primers and probes used for the qPCR are listed in Supplementary Table 1.

BBB Leakage Analysis

At 5 dpi, animals were anesthetized and 100 μL of FITC-Dextran were injected i.v. (ThermoFisher Scientific D3306, 5 mg/mL). After 1 h, the brains were removed and immediately frozen at -80°C . About 30 μm brain slices were prepared using a cryostat. Epifluorescence images were directly taken for quantification of FITC fluorescence or briefly postfixed for 30 min using 4% PFA, washed once with PBS and stained with anti-mouse immunoglobulin G (IgG) coupled to Alexa Fluor A647 (115-606-072, Dianova, Germany, 1:500) for 2 h and DAPI for 5 min. After mounting and drying of sections, confocal images were taken using constant exposure settings. Single channel maximum intensity projections were subjected to automatic threshold and used for quantifications of the fluorescent area using NIH ImageJ software.

Statistical Data Analysis

Confocal laser scanning (Zeiss LSM5; Zeiss LSM710) microscope was used to quantify immunopositive cells in sections or cell culture. For each of the quantifications, at least 3 animals or experimental culture batches were examined. All quantifications

of immunohistochemistry were based on analysis of at least 5 sections per animal. Statistical analyses of data were performed using the GraphPrism 5.0 software. Data were tested for the normal distribution using the Kolmogorov–Smirnov test, and significance between means from 2 experimental groups was analyzed using 2-tailed unpaired Student's *t*-test and between multiple groups by one-way analysis of variance (ANOVA) analysis. All values were plotted as mean \pm standard error of the mean (SEM), unless otherwise stated. Significance is indicated as * ($P < 0.05$), ** ($P < 0.01$), and *** ($P < 0.001$).

Results

Age-Related Changes in Astrocytes within the GM of the Somatosensory Cerebral Cortex

Given previous evidence for changes in astrocytes during physiological aging in human or rodent brains (Orre et al. 2014; Rodriguez et al. 2014), we first investigated whether the process of aging is associated with phenotypical changes in astrocytes of the somatosensory GM in 3 experimental cohorts of mice: young (2–3 months of age), middle-aged (6–9 months of age), and old (12–18 months of age). Similar to observations in other regions of the cerebral cortex (Rodriguez et al. 2014), aging induced a progressive increase of GFAP-immunopositive astrocytes also in the somatosensory GM (Fig. 1A). Interestingly, the total number of astrocytes labeled by S100 β remained the same, while the proportion of GFAP+ astrocytes increased by nearly 3-fold between 2 and 18 months of age (Fig. 1B). The aging process induced not only a significant increase of GFAP+ astrocytes but also changes in their morphology (Fig. 1C,D). In contrast to the resting morphology of the Aldh111 immunopositive but GFAP-immunonegative in the somatosensory GM, which remained comparable at all age stages studied, the population of Aldh111+GFAP+ astrocytes showed hypertrophy with age (Fig. 1D). The age-related development of the activated astrocyte phenotype is further corroborated by changes at the transcriptional level, as determined by quantitative RT-PCR of mRNA from GFAP-mRFP1+ astrocytes sorted by FACS from the somatosensory GM of young and old transgenic mice (see Supplementary Fig. 1A,B). Indeed, RFP+ cells isolated from old animals showed not only higher expression levels of GFAP mRNA than those in young mice (see Supplementary Fig. 1A), but also elevated levels of STAT3 mRNA (see Supplementary Fig. 1B). These data suggest that age-induced upregulation of STAT3-dependent mechanisms, known to play a critical role in activation of astrocytes and upregulation of GFAP expression after injury (Sriram et al. 2004; Herrmann et al. 2008; Sofroniew 2009; O'Callaghan et al. 2014; Levine et al. 2016) may contribute to the higher GFAP levels in aging.

Since the activated state of astrocytes is regarded as sign of reactive astrogliosis, a process during which a subset of astrocytes can acquire a proliferative phenotype (Simon et al. 2011; Sirko et al. 2013), we wondered whether astrocytes might also resume proliferation during normal aging. In order to immunolabel proliferating astrocytes, we supplied the nucleotide analog-BrdU for 5 days in drinking water. Of note, the very few BrdU+ astrocytes detectable in the cerebral cortex GM of 2-month-old mice (Simon et al. 2011; Sirko et al. 2013) became even fewer with aging, such that starting with 12 months of age, virtually no BrdU+GFAP+ cells were detected in the somatosensory GM (see Supplementary Fig. 1D). Notably, also the proliferative activity of other glial cell types, such as NG2+ glia or Iba1+ microglia, was not increased with aging. In

contrast to astrocytes, these glial cell types did not, however, exhibit hypertrophy or an activated morphology (Supplementary Fig. 1E,F). Thus, although astrocytes acquire a partially activated phenotype, neither they nor other glial cells increased their proliferation during normal aging.

Effect of Aging on Astrocyte Numbers and Homeostasis after Traumatic Injury

Considering the age-associated changes in the GM astrocytes, we also investigated the effects of aging on astrocyte reaction to the stab wound injury in this region. In all experimental groups, a stab wound induced heterogeneous astrocyte reactions in the GM parenchyma, including hypertrophy, substantial upregulation of GFAP, and polarization toward the wound site (Fig. 2A). To investigate whether there are age-related differences in the morphological phenotype of reactive astrocytes in proximity or distance to the lesion core, we used double staining with GFAP and Aldh111. At 5 dpi, the morphology of reactive astrocytes within the post-traumatic GM was not uniform and varied with proximity to the lesion in both young and old brains (Fig. 2B,C). However, there were obvious differences between age groups. For instance, reactive astrocytes located in close proximity to the lesion (within 300 μ m) in old mice exhibited a clear reduction of GFAP-immunoreactivity and less complex processes compared with those in young animals (Fig. 2C). Irrespective of age, with increasing distance from the lesion, astrocytes in the post-traumatic GM transitioned gradually to their bushy morphologies with fine branching processes. Although most astrocytes within the penumbra gradually reverted to their basic domain structure, there were some cases in which elongated processes from activated astroglia entered domains of neighboring astrocytes (Fig. 2C). However, in contrast to the young animals, where cortical astrocytes exhibited almost undetectable levels of GFAP starting with \sim 550 μ m distance to the lesion, the radius of the area covered by GFAP-immunoreactivity in old animals was significantly increased ($712 \pm 64 \mu$ m vs. $545 \pm 56 \mu$ m in 18-month-old vs. 2 month-old animals respectively; $P = 0.011$). This age-related enlargement of astrogliosis was not linked to morphological alterations in aged astrocytes, as over long distances to the lesion (\geq 400 μ m) the appearance, shape or length of elongated processes of Aldh111+ astrocytes was well comparable between young and old animals, but rather with the retained upregulation of GFAP in aged astrocytes located even at an 800 μ m distance to the lesion (Fig. 2B,C).

Despite an overall increased spread of astrogliosis in the post-traumatic GM of aged animals, the density of GFAP+ cells within the 300 μ m wide region surrounding the lesion core appeared to decrease with age (Fig. 2B,C and E). With distance from the lesion core, however, this prominent gradient of diminishing density of astroglial cells gradually transitioned to a density similar to that seen in healthy GM tissue of the aged brain (Fig. 2C). Consistent with the age-related decrease in density of GFAP+ cells in the area adjacent to the lesion and reduction of GFAP+ profiles of aged reactive astrocytes, also the expression levels of GFAP mRNA in astrocytes sorted from the somatosensory GM of 18-month-old Aldh111-eGFP transgenic mice at 5 dpi was strongly decreased compared with Aldh111-eGFP+ astrocytes from young animals at the same time point after injury (Fig. 2J). That was different in young animals where the population of GM astrocytes lost upon stab wound injury was nearly replaced during the first 5 days after injury (compare Fig. 1B vs. 2D), suggesting that the ability to recover the astroglial population in the post-traumatic GM decreases in the older brain.

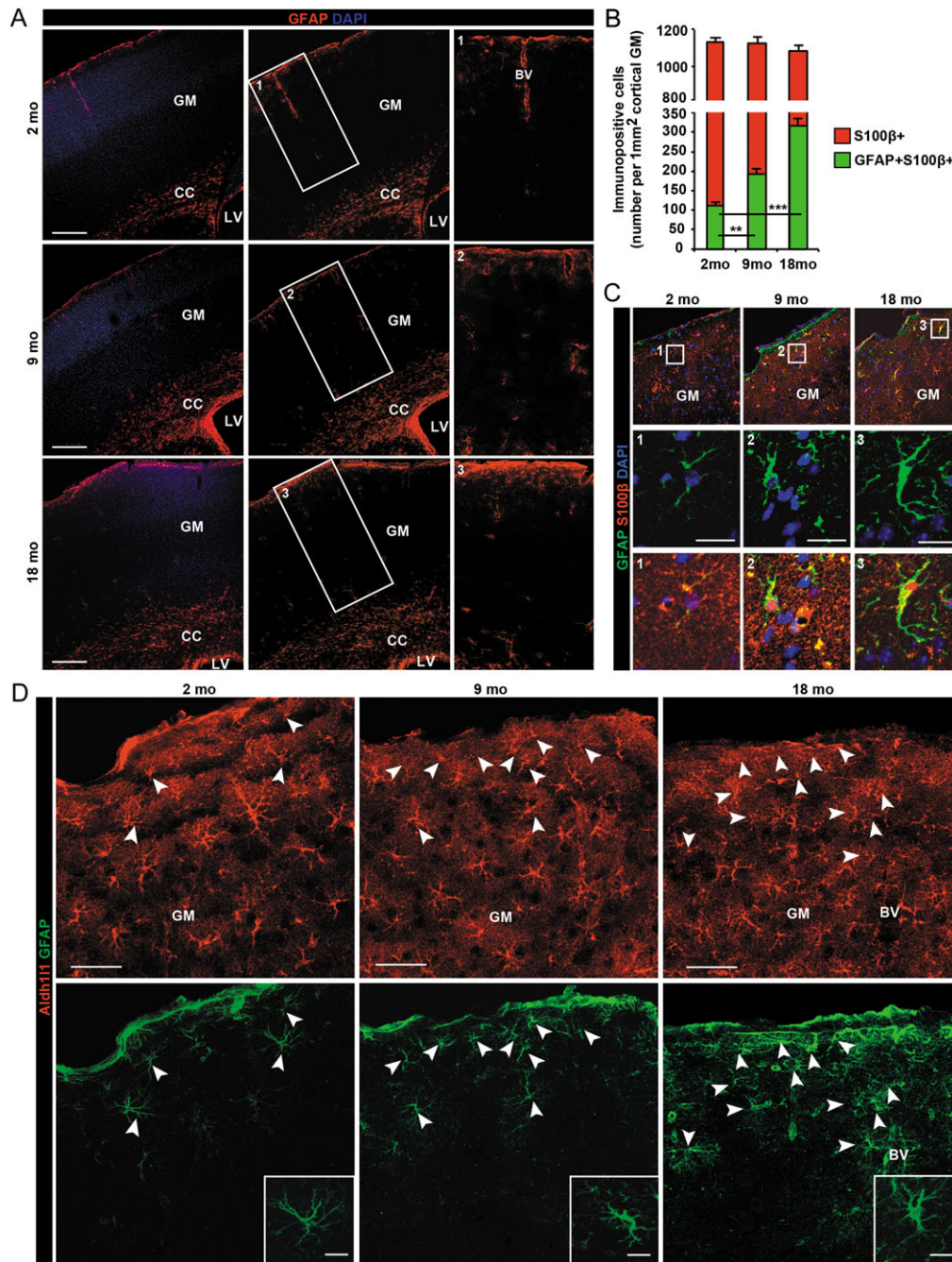


Figure 1. Age-associated changes in astroglial population within the intact somatosensory GM. (A) Distribution of GFAP-immunopositive astrocytes in the intact fore-brain of mice at 2, 9, and 18-month of age. High magnification images of the somatosensory GM correspond to the boxed regions (1–3). (B) Quantification of S100β+ and GFAP+S100β+ cells within the somatosensory GM of young (2-month-old) and aged mice (18-month-old) indicates significant increase in the number of GFAP+ cells in relation to normal aging, while the population of S100β+ astrocytes in this region of cerebral cortex remains unchanged. (C) Immunostaining of frontal brain sections for GFAP and S100β showing a progressive change in both the frequency and morphology of GFAP+ cells, which are mostly located in the upper layer of the somatosensory GM. High magnification images (1–3) correspond to the boxed regions and illustrate morphological changes in astroglial cells with age. (D) In contrast to Aldh1l1+GFAP- astrocytes, the population of GFAP+ astrocytes (white arrowheads) in the somatosensory GM showed cellular hypertrophy with age. High magnification images showing the changes in astroglial GFAP-profile during the process of aging. Cell nuclei were counterstained with DAPI. Data are plotted as mean ± SEM from $n \geq 3$ independent experiments. Significance between means was analyzed using 2-tailed unpaired Student's t-test or between multiple groups by 1-way ANOVA test and indicated as *P-value < 0.05, **P-value < 0.01, and ***P-value < 0.001. Scale bars: 200 μm in (A), 100 μm in (D), 75 μm in (C), and 20 μm in boxes.

Age-Related Impairment of Proliferative Astrocyte Response to Traumatic Injury

Since proliferation appears to be the only way to restore astrocyte numbers in the injured cerebral cortex (Bardehle et al. 2013),

the impaired restoration of normal astrocyte numbers after GM injury in old animals may be due to failure of aged astrocytes to either appropriately initiate or maintain their proliferative response. Given that reactive astrocytes in young adult animals reach their peak of proliferation at 5 dpi (Sirko et al. 2009, 2015),

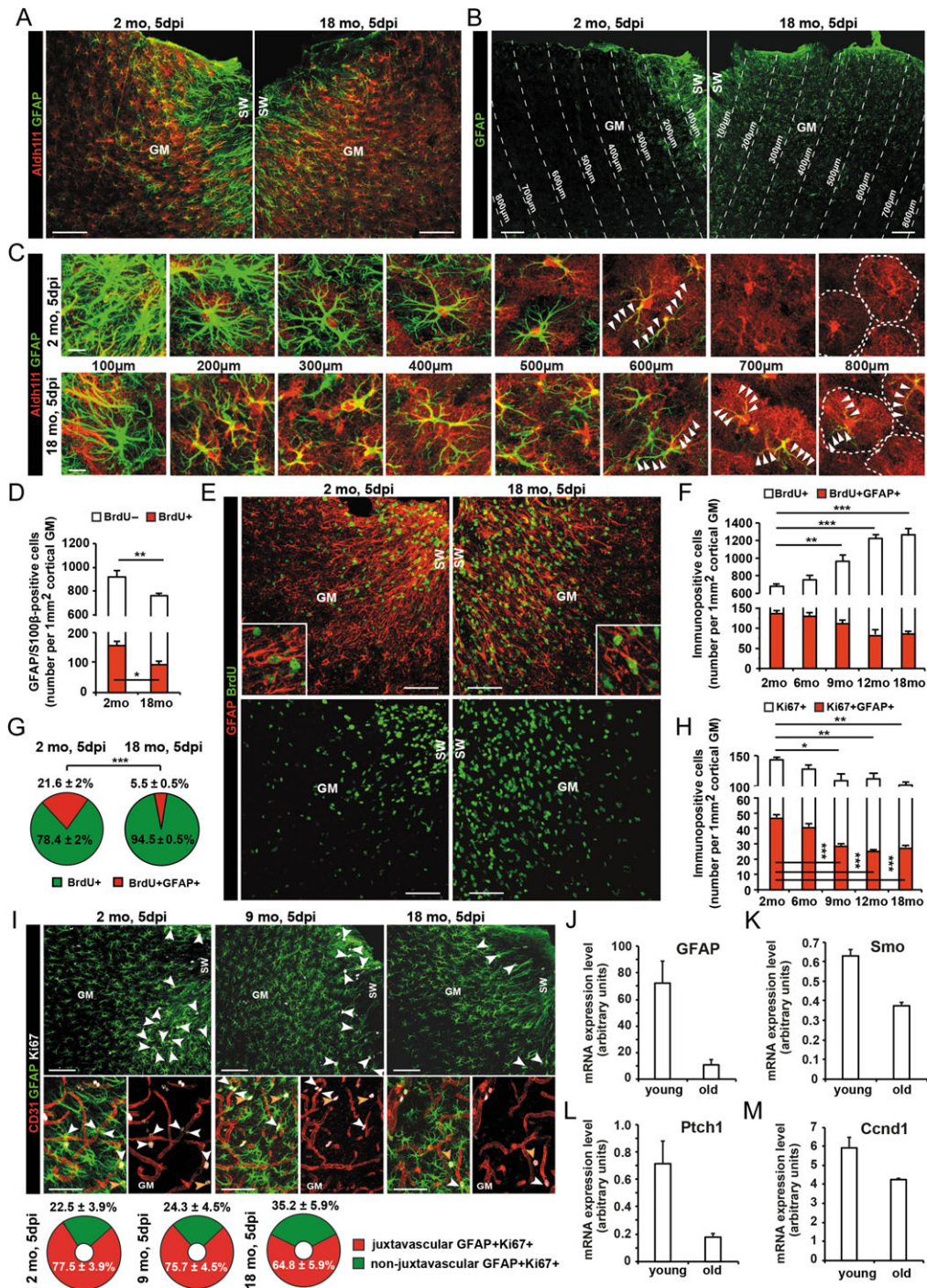


Figure 2. Age-dependent changes in proliferative astrocyte response to the stab wound injury of the GM. (A) Stab wound injury of the somatosensory GM induced a broad expression of GFAP in parenchymal astrocytes at the injury site, as demonstrated by immunostaining with GFAP and Aldh1l1 at 5 dpi. (B) Representative overview images reveal distribution of GFAP+ astrocytes in the penumbra of young and old mice at 5 dpi. Note that the region covered by GFAP+ immunoreactivity in the injured cerebral cortex of 18-month-old animals was larger compared with 2-month-old animals, but the tissue in the close vicinity to the lesion in old mice contain a lower density of GFAP+ astrocytes than in young ones. (C) The fluorescence micrograph panels reveal the morphological changes in astroglial cells at different distance to the injury site at 5 dpi, as indicated in B. Note that the morphological appearance of GFAP+ astrocytes located in the close proximity to the lesion (within 300 μ m) in old animals was reduced. With increasing distance from the lesion core, some bushy astrocytes exhibited fine GFAP+ cell processes (white arrowheads) within the individual domains (as indicated by the dashed line), even at a long distance to the lesion (~800 μ m). (D) At 5 dpi, absolute numbers of GFAP+S100 β +BrdU+ cells within the parenchyma adjacent to injury site (within 300 μ m) decreased significantly with aging. (E) Immunostaining reveals an age-related expansion of the BrdU+ cell pool and depletion of reactive astrocytes entering the cell-cycle (BrdU+GFAP+) in the injured GM parenchyma throughout 5 days after injury. (F) A progressive depletion of the proliferating astrocyte pool over the course of aging occurs concomitantly with an increase in absolute numbers of BrdU+ cells within the individual GM. (G) Pie charts show the significantly reduced proportion of GFAP+BrdU+ cells almost all cycling (BrdU+) cells in the injured GM of 18-month-old mice compared with 2-month-old animals at 5 dpi. (H) Statistical analysis of Ki67+ and Ki67+GFAP+ cell numbers in the penumbra of aged mice at 5 dpi. (I) The majority of Ki67+GFAP+ cells within 500 μ m of the injured GM in 2-, 9-, and 18-month-old mice were located at the surface of vessels (CD31+) (white arrowheads). Note that the bias of reactive astrocytes to proliferate at the interface of blood vessels remained unaffected by aging, as in all groups of animals the majority

when proliferation of microglia and NG2+ glia has already decreased (Simon et al. 2011), the age-dependent effect on the entire cycling pool of reactive astrocytes was examined by continuous administration of BrdU for 5 days, starting at 2 h after injury. At this time point after injury, the number of proliferating astrocytes in the penumbra of old compared with young mice was reduced by ~40% (Fig. 2D–E). This decreased proliferative activity was rather specific for astrocytes, as the total pool of BrdU+ cells strikingly increased with aging (Fig. 2E), and was nearly doubled in the penumbra of 18-month-old mice compared with young mice (Fig. 2F). Notably, the majority of BrdU+ cells in the injured GM of old animals were microglia, whose proliferation increased significantly ($60.0 \pm 1.9\%$ vs. $77.5 \pm 2.1\%$ of BrdU+Iba1+ among all BrdU+ cells within the injured GM of 2-month-old vs. 18-month-old animals, respectively; $P = 0.0003$) (see Supplementary Fig. 2A,B), while the proliferation of astrocytes and NG2+ glia decreased with aging ($20.1 \pm 1.9\%$ vs. $8.8 \pm 1.4\%$ of BrdU+NG2+ among all BrdU cells within the injured GM of 2-month-old vs. 18-month-old animals, respectively; $P = 0.0001$). Indeed, the contribution of proliferating astrocytes (BrdU+GFAP+) was reduced to ~6% of all cells that proliferate within the first 5 days after injury in 18-month-old mice, compared with ~22% in young animals (Fig. 2G).

We proceeded to examine the cells dividing at 5 dpi by labeling for Ki67. Notably, opposed to cells labeled with BrdU for the entire time after injury, the total number of Ki67+ cells was significantly decreased in an age-dependent fashion, starting already at 9 months of age (Fig. 2H). Compared with young mice, the total pool of Ki67+ cells at 5 dpi in 18-month-old mice shrank by ~30%, and for GFAP+Ki67+ this effect was ~40% (Fig. 2H,I). Interestingly, however, the bias of reactive astrocytes to proliferate at the interface of blood vessels remained unaffected by aging, as in all groups of animals the majority of Ki67+GFAP+ cells within the injured GM was found at juxtavascular positions (Fig. 2I). Thus, the glial population that had an increased proliferative response in the aged brain, namely microglia, did not show prolonged proliferation (see Supplementary Fig. 2C). Rather, the proliferative response in the old GM is decreased at 5 dpi, including a significant decrease in reactive astrocyte proliferation.

Modulation of Sonic Hedgehog Signaling can no Longer Boost Proliferation of Reactive Astrocytes in the Injured GM of Aged Mice

Given that the deficits in proliferative behavior of cells in the aging brain, e.g., neural stem cells (NSCs), have been shown to be caused by reduced niche signals (e.g., growth factors and cytokines) (Galvan and Jin 2007; Lee et al. 2012; Yun et al. 2015), we aimed to determine to which extent providing such signals could rescue the age-related decline in reactive astrocyte proliferation. As Sonic hedgehog (Shh) signaling is a potent regulator of astrocyte proliferation following injury (Bambakidis et al. 2012; Sirko et al. 2013), acting directly on reactive astrocytes in young adult mice (Sirko et al. 2013), we investigated whether the Smoothened (Smo) agonist SAG was sufficient to boost proliferation of reactive astrocytes in the penumbra of older mice.

Similar to observations in young adults, a daily systemic application of SAG significantly increased the number of Ki67+ cells also in the injured GM of middle-aged and old animals (Fig. 3A, B and D). Surprisingly, however, this effect was not exerted on astrocytes in old animals, as the number of Ki67+GFAP+ cells in the penumbra of these animals was not significantly increased upon treatment with SAG (28.9 ± 1.7 vs. 35.3 ± 2.2 Ki67+GFAP+ cells/mm² injured GM of 18-month-old untreated vs. SAG-treated animals, respectively; $P = 0.19$) (Fig. 3C,D). Furthermore, reactive astrocytes contributed only to $20.1 \pm 1.5\%$ of the total Ki67+ cell pool labeled in the GM of old SAG-treated mice at 5 dpi, in contrast to young SAG-treated mice with $39.2 \pm 1.7\%$ GFAP+ of all Ki67+ cells. Thus, reactive astrocyte proliferation is not only higher in the injured GM of young and middle-aged mice, but also particularly boosted by SAG, while after 9 months of age proliferation of reactive astrocytes is much lower and no longer susceptible to the boosting effect of SAG (Fig. 3D).

Given the accelerated astrocyte reaction in aged poststroke rodents (Badan et al. 2003) and the fact that astrocytes at 5 dpi could not be stimulated to increase proliferation in the old brains, we wondered if SAG would increase their proliferation at earlier stages after injury. Therefore, we used again the continuous BrdU labeling for the entire 5 days after injury to detect any cell proliferation changes in response to an enhanced Shh signaling (Fig. 3A,B). Application of SAG caused a significant increase in BrdU+GFAP+ cells within the penumbra of young and middle-aged animals, but the number of BrdU+ astrocytes in old SAG-treated mice was not significantly higher than in the age-matched vehicle-treated controls (Fig. 3E). Indeed, only $10.5 \pm 0.9\%$ of all GFAP-labeled astrocytes proliferated within the entire 5 days after injury, while this fraction was $20.6 \pm 1.9\%$ in young SAG-treated animals. In total, the number of BrdU+GFAP+ cells was reduced by nearly 30% in the penumbra of SAG-treated animals between 2 and 18 months (217.9 ± 15.9 vs. 156.1 ± 12.9 BrdU+GFAP+ cells/mm² injured GM of 2- and 18-month-old mice, respectively).

Thus, the proliferation of reactive astrocytes in older animals could not be boosted at any time point after injury by SAG-mediated stimulation of the Shh pathway, suggesting that either other factors are missing in the injury environment or cell-intrinsic changes are responsible for the substantially diminished proliferative subset of reactive astrocytes in aged animals. In this context, we also noted a clear trend toward age-related downregulation of the mRNA levels of Shh transducer Smothened (Smo), Shh receptor Patched (Ptch1) and their effector cyclin D1 (Ccnd1) in GFP+ astrocytes purified from young and old Aldh111-eGFP mice at 5 dpi (Fig. 2K–M). These data imply an interference with Shh pathway in aged reactive astrocytes.

Age-Dependent Reduction of Proliferating Reactive Astrocytes in Vitro

To minimize the effect of the environment, we decided to analyze cell divisions of reactive astrocytes by single-cell imaging in vitro. Because the extent of astrocyte proliferation in vivo does not significantly change between 12 and 18 months of

of Ki67+GFAP+ cells within the injured GM was found at juxtavascular positions. (J–M) Bar graphs depicting levels of the mRNAs determined by qRT-PCR in GFP+ cells purified by FACS from young and old Aldh111-GFP mice at 5 dpi (data are plotted as mean \pm SEM of technical triplicates per separate age-groups of animals, as described in Material and Methods section). All data in D, F, G, H, and I are plotted as mean \pm SEM from $n \geq 3$ experiments. Significance between means was analyzed using 2-tailed unpaired Student's *t*-test or between multiple groups by 1-way ANOVA test and indicated as **P*-value < 0.05, ***P*-value < 0.01, and ****P*-value < 0.001. Cell nuclei were counterstained with DAPI. Scale bars: 100 μ m in (A, B, and E), 75 μ m in (J) and 15 μ m in (C).

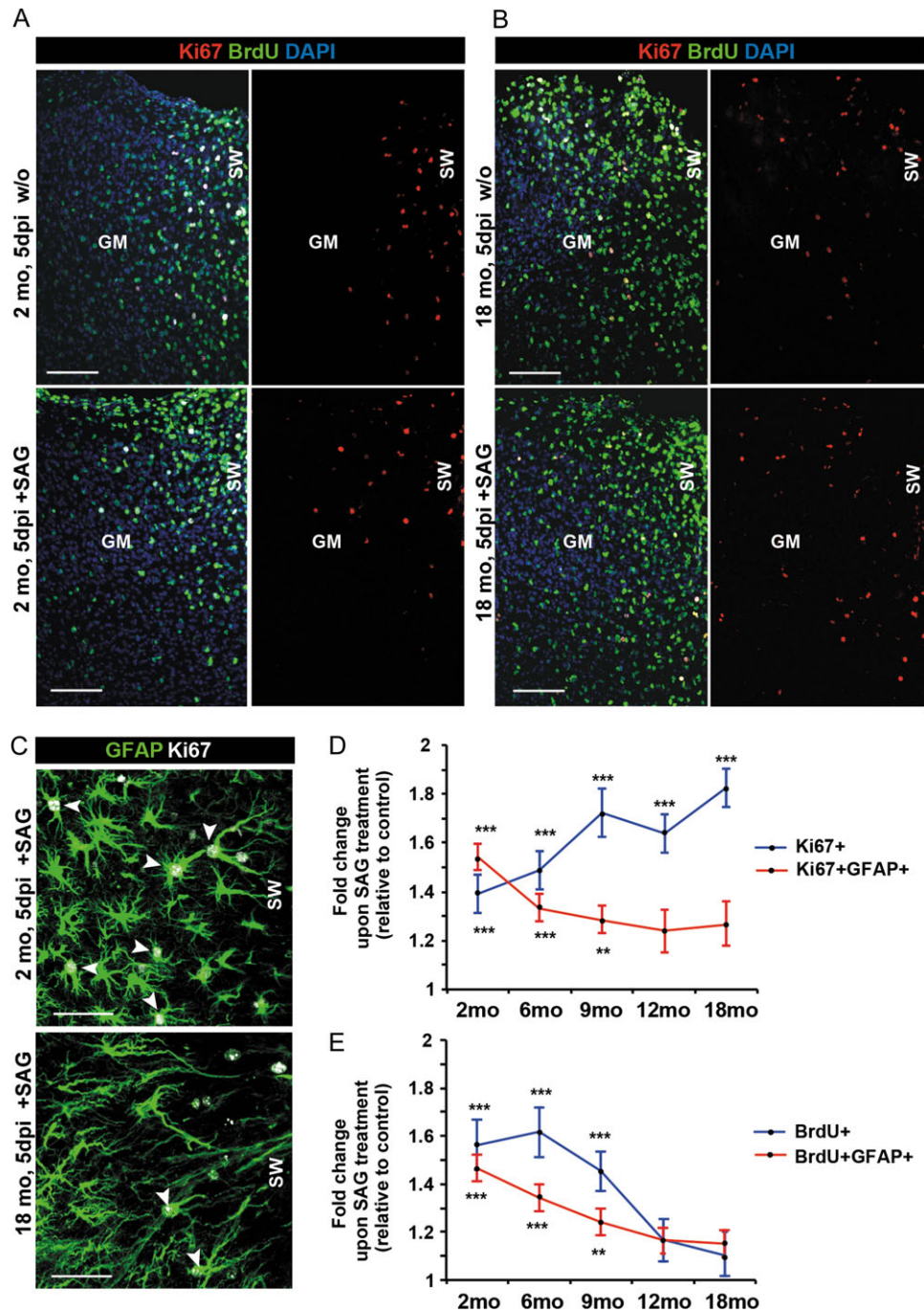


Figure 3. Modulation of Shh signaling can no longer boost proliferation of reactive astrocytes in the injured GM of aged mice. (A, B) Immunostaining with BrdU and Ki67 revealed that *in vivo* application of SAG modulated proliferative response of cells within the injured GM of young and old animals. (C) SAG-treatment *in vivo* modulated the injury-induced astrocyte proliferation in young animals, but was not sufficient to boost the proliferative activity in reactive astrocytes in old mice. (D) Age-related changes in the numbers of Ki67+ cells and the reciprocal relationship between the numbers of Ki67+GFAP+ cells and the age of animals. (E) The incidence of BrdU+ cells after application of SAG was significantly elevated in young and middle-aged, but not in old animals, where the majority of BrdU+ cells was GFAP negative. All data are plotted as mean \pm SEM from $n \geq 3$ experiments. Significance between means was analyzed using 2-tailed unpaired Student's *t*-test or between multiple groups by one-way ANOVA test and indicated as **P*-value < 0.05, ***P*-value < 0.01, and ****P*-value < 0.001. Cell nuclei were counterstained with DAPI. Scale bars: 75 μ m in (A, B), 100 μ m in (C).

age, cell cultures of reactive glia were prepared from the injured somatosensory GM of 2-, 6-, and 12-month-old animals at 5 dpi. These cultures contained several cell types, but were highly enriched for astrocytes and microglia, while only few oligodendroglial cells (~5%) and no neurons were found. Indeed, at the starting point of live imaging, GFAP+ astrocytes together

with Iba1+ microglia comprised two-thirds of all adherent cells, with no significant differences between cultures prepared from young and old brains ($35.3 \pm 1.9\%$ and $30.9 \pm 2.5\%$ of GFAP+ cells and $40.2 \pm 2.2\%$ and $43.8 \pm 2.0\%$ of Iba1+ cells in the cell cultures from 2- and 12-month-old mice, respectively; $n = 3$, $P = 0.177$, and $P = 0.221$). As neither the growth profile of cell

populations (see in Materials and Methods section) nor their composition significantly varied among reactive glia cultures, these culture conditions are largely comparable.

To directly visualize dividing reactive astrocytes, we took advantage of fluorescent ubiquitylation-based cell-cycle indicator (FUCCI)-S/G2/M-mAG-hGeminin mice (Sakaue-Sawano et al. 2008), which we bred with transgenic GFAP-mRFP1 mice (Hirrlinger et al. 2005). The dual-color fluorescence enabled us to detect reactive astrocytes (GFAP-RFP+) in S/G2/M phases of

cell cycle by expression of FUCCI (mAG-hGeminin+) (Fig. 4A). Continuous single-cell live imaging (Costa et al. 2011; Ortega et al. 2013) further allowed us to follow the progeny of reactive astrocytes for 7 days in vitro (div) (Fig. 4B,C).

Single-cell tracking analysis revealed that regardless of age, the majority of GFAP-RFP+/mAG-hGeminin+ cells (95%) divided within 36 h (Fig. 4D,E) and they remained in the astrocyte lineage, as their progeny were all GFAP+ but not β III-tubulin+ neurons or O4+ oligodendrocytes (Fig. 4C). However, single

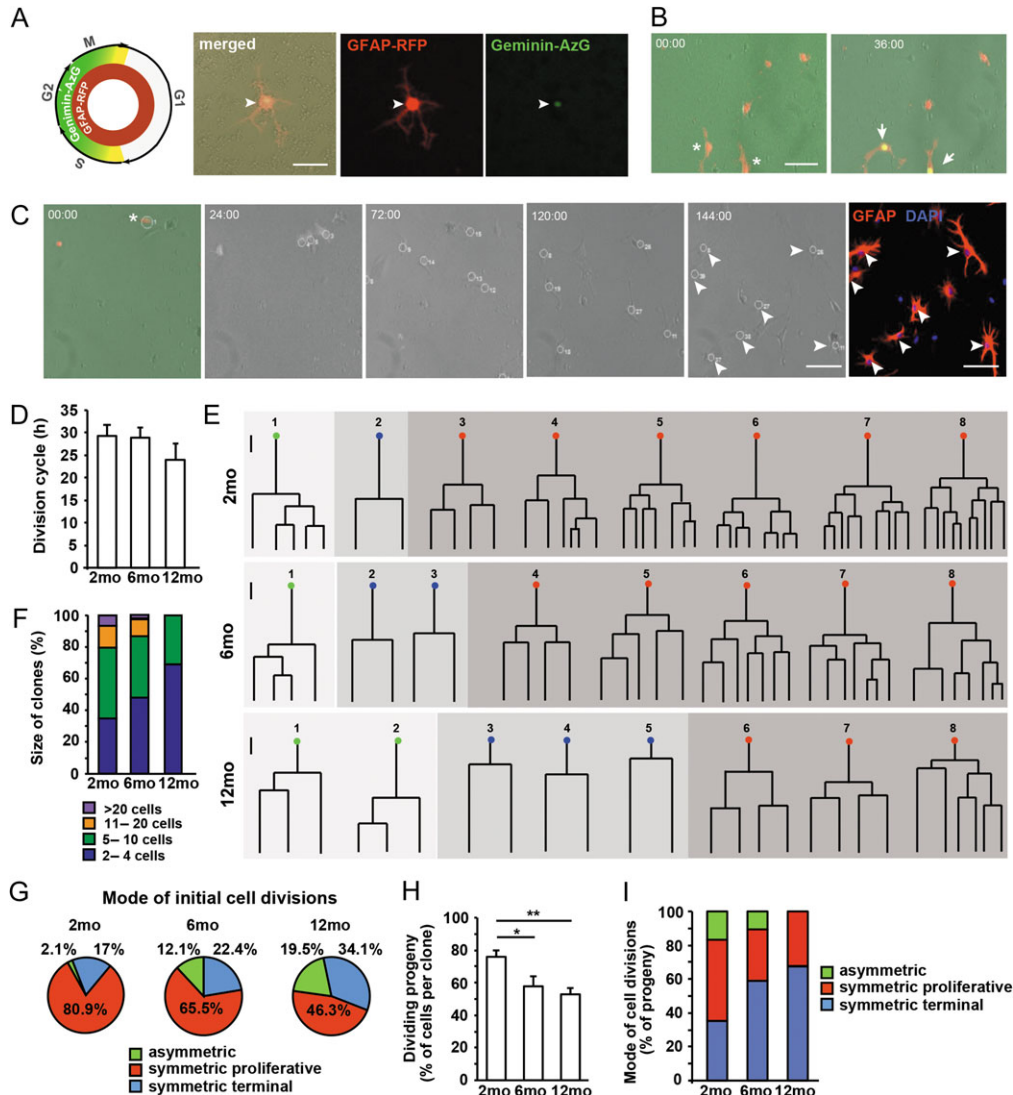


Figure 4. Age-related bias in the mode of cell divisions in aged reactive astrocytes and their progeny. (A) Scheme depicting the relationship between the cell-cycle phases and expression of fluorescent protein Azami-Green (mAG)-tagged Geminin (green) in RFP-GFAP+ (red) reactive astrocytes during S/G2/M phases of the cell cycle. A representative example shows GFAP+/Geminin+ astrocyte in cell culture prepared from the injured GM of 2-month-old mice at 5 dpi. (B) After plating in the adherent culture condition, proliferating GFAP-RFP+ cells (arrowheads) were distinguishable by expression of mAG-tagged Geminin (arrows). (C) Sequences of time-lapse images revealed generation of cell colony from a single GFAP-RFP+/mAG-hGeminin+ cell at different time points in vitro. Post-imaging of immunolabeled cells demonstrate that almost all generated daughter cells were GFAP+ (arrowheads). (D) Quantification of the average length of division cycle revealed no significant differences in cell-cycle length of proliferative astrocytes isolated from different age-groups of the injured animals. (E) Examples of lineage trees obtained from single dividing GFAP-RFP+/mAG-hGeminin+ cells show that proliferating astrocytes from each age-group of animals were capable to divide asymmetrically (light gray box), symmetrically terminal (darker gray box), or proliferative (dark gray box) in vitro. (F) The number of cells per colony generated from single GFAP-RFP+/mAG-hGeminin+ cell revealed substantial age-related differences, as shown by the frequency of clones at a given size among all clones generated. (G) Pie charts showing the percent of asymmetrically, symmetrically terminal or proliferative dividing GFAP-RFP+ astrocytes obtained from 2-, 6-, and 12-month-old animals at 5 dpi. (H) The proportion of proliferating progeny generated from GFAP-RFP+/mAG-hGeminin+ cell per cell clone decreased with aging. (I) The frequency of asymmetrically, symmetrically terminal or proliferative dividing progeny of GFAP-RFP+/mAG-hGeminin+ cells revealed that reactive astrocytes lost their self-renewal capacity in an age-dependent manner and divided predominantly symmetrically terminal with increasing age of animals. All data are plotted as mean \pm SEM from $n \geq 3$ independent experiments. Significance between means was analyzed using 2-tailed unpaired Student's *t*-test or between multiple groups by one-way ANOVA test and indicated as **P*-value < 0.05, ***P*-value < 0.01, and ****P*-value < 0.001. Scale bars: 20 μ m in (A–C).

proliferating astrocytes from the injured GM of young mice generated a higher number of larger clones (>10 cells/clone) than those from old animals (Fig. 4E,F).

Lineage tree analysis of individual GFAP-RFP+/mAG-hGeminin+ cells showed that this was due to changes in their cell division patterns, which we defined based on the proliferation of the daughter cells. Although reactive astrocytes from each age group were capable of dividing symmetrically and asymmetrically (see Supplementary Movie 1–3), there were notable age-related changes in the frequency of certain cell division modes (Fig. 4G). For instance, the primary mode of the initial division of young reactive astrocytes was symmetric proliferative (81%, 38/47), resulting in the generation of 2 proliferating daughter cells (Fig. 4E, G). Only 17% (8/47) of the initial divisions were terminal divisions with the daughter cells no longer dividing during the observation time and only 2% (1/47) dividing asymmetrically, generating one proliferating and 1 non-proliferating daughter cell (Fig. 4E,G). Under the same culture conditions, the proportion of symmetric proliferative GFAP/RFP+ cells was, however, much reduced for cells from older animals and comprised 66 or 46% of all reactive astrocytes isolated from middle-aged or old animals, respectively (Fig. 4E,G). Conversely, symmetric terminal divisions were increased to 22% (13/58) or even 34% (19/41) of all initial reactive astrocyte divisions in reactive astrocyte cultures from the injured middle-aged or old cerebral cortex GM, respectively (Fig. 4E,G). Given that terminal cell division produces 2 nonproliferative daughter cells, a 2-fold increase in terminally dividing GFAP/RFP+/mAG-hGeminin+ cells isolated from 2 or 12-month-old animals indicated a prominent age-related shift toward cell-cycle exit, and hence, age-induced reduction in the number of cells generated from a single reactive astrocyte (Fig. 4H). This was also reflected in a progressive age-related reduction in repetitive divisions of reactive astrocytes, as many of them divided in symmetric terminal mode already at the first division (Fig. 4G). Conversely, the progeny of young mAG-hGeminin+ reactive astrocytes underwent up to 4 rounds of divisions and produced a relatively large number of proliferating cells before exiting the cell cycle (Fig. 4E,H,I).

During analyses of time-lapse data, we also noted that progeny cells produced through 66% of all recorded divisions of aged GFAP/RFP+/mAG-hGeminin+ astrocytes underwent cell death, while in young or middle-aged cultures it was the case in 54% or 51% of reactive astrocyte divisions, respectively. Moreover, also the average ratio of dying-to-surviving progeny cells increased with age of dividing astrocytes (9% : 91% vs. 14% : 86% vs. 16% : 84% in the cell cultures from 2-, 6-, and 12-month-old mice, respectively). It is important to note, that irrespectively of age, cell death occurred more frequently through progeny produced by non-terminal divisions of GFAP/RFP+/mAG-hGeminin+ cells, and there was a positive correlation between the number of cell divisions elapsed and the rate of cell death. On average $10.8 \pm 2.1\%$ of non-surviving progeny tend to undergo cell death after their first divisions, while $26.2 \pm 5.9\%$, $29.1 \pm 6.0\%$, and $33.9 \pm 5.1\%$ of them die after second, third, and fourth cell division rounds, respectively. Together, these findings provide strong evidence in support of the notion that age-related changes to the proliferative program significantly diminish the reproductive ability of reactive astrocytes and together with reduced viability in their progeny lead to the depletion of the subset of proliferating reactive astrocytes with age. Given these significant differences in the behavior of young and aged proliferating reactive astrocytes in an identical environment *in vitro*, it is likely that age-related changes to the proliferative astrocyte response reflect the changes at the cell-intrinsic level.

Reactive Astrocytes from the Aged GM Fail to Resume the Symmetric Proliferative Mode of Division in Response to Modulation of the Shh Signaling

Next, we aimed to examine how Shh signaling may influence the mode of division of reactive astrocytes isolated from younger animals, and whether reactive astrocytes from older animals may at all react to Shh signaling, e.g., by changing the mode of their division. Interestingly, addition of SAG to the culture medium led to a huge expansion of clones derived from single astrocytes isolated from young mice (Fig. 5A and see Supplementary Movie 4). This reaction was already much attenuated for cells from 6-month-old mice and entirely absent for reactive astrocytes from 12-month-old mice (10.3 vs. 2.1% of clones containing >20 cells in SAG-treated cultures from young vs. old injured mice, respectively; Fig. 5B,D).

Since the ability to form larger colonies could be due to the shortening of cell-cycle length, we measured the time between cell divisions. Indeed, when compared with control cultures of the same age, SAG-treatment significantly accelerated the cell-cycle time of young reactive astrocytes and their progeny (29.7 ± 2.8 h vs. 21.8 ± 1.3 h in control vs. SAG-treated cultures, respectively, $P = 0.017$). Conversely, the cell-cycle length of reactive astrocytes derived from old animals remained unchanged (24.5 ± 2.9 h vs. 23.3 ± 1.8 h in control vs. SAG-treated cultures, respectively). It is, however, noteworthy, that the cycle length without SAG addition is not slower for reactive astrocytes derived from old animals indicating that the failure to produce more progeny is not due to age-related differences in cell-cycle length, but rather the mode of division and the ability of their progeny to re-enter the cell-cycle (Fig. 5C,D). Therefore, we next analyzed to what extent re-entry into cell cycle was affected by SAG addition to the cultures of reactive astrocytes isolated from young and old mice. Indeed, the direct progeny of young GFAP-RFP+ cells underwent up to 6 rounds of cell division in the SAG-containing culture, thereby massively amplifying the pool of dividing progeny derived from a single proliferative astrocyte (Fig. 5B,D). Although enhanced Shh signaling was sufficient to mediate proliferative divisions in young reactive astrocytes, it was not sufficient to do so in aged reactive astrocytes (Fig. 5B,C). Indeed, in presence of SAG ~90% of progeny derived from the young GFAP-RFP+/mAG-hGeminin+ cells were dividing in a symmetric or asymmetric proliferative mode, while this proportion was already diminished to 60% for astrocytes derived from 6-month-old animals. At 12 months of age, only one-third of the astrocyte progeny underwent proliferative division, and modulation of the Shh pathway did not increase this proportion (Fig. 5E). Likewise, SAG could not elicit repetitive divisions of astrocytes from 12-month-old mice, as only 2% were able to undergo more than 3 rounds of divisions. Thus, the effects of SAG-treatment are due to the shortening of cell-cycle length and a strongly increased re-entry into cell cycle of astrocytes from young adult mice, but remain without effects even *in vitro* for proliferating astrocytes from older mice.

Alteration of Injury-Induced Stem Cell Response in Aging

As proliferation of reactive astrocytes goes hand in hand with the acquisition of stem cell potential determined by generation of self-renewing neurospheres (Buffo et al. 2008; Sirko et al. 2009, 2013), we investigated the consequences of the above described age-related decrease in astrocyte proliferation on their injury-induced stem cell capacity that was assayed by

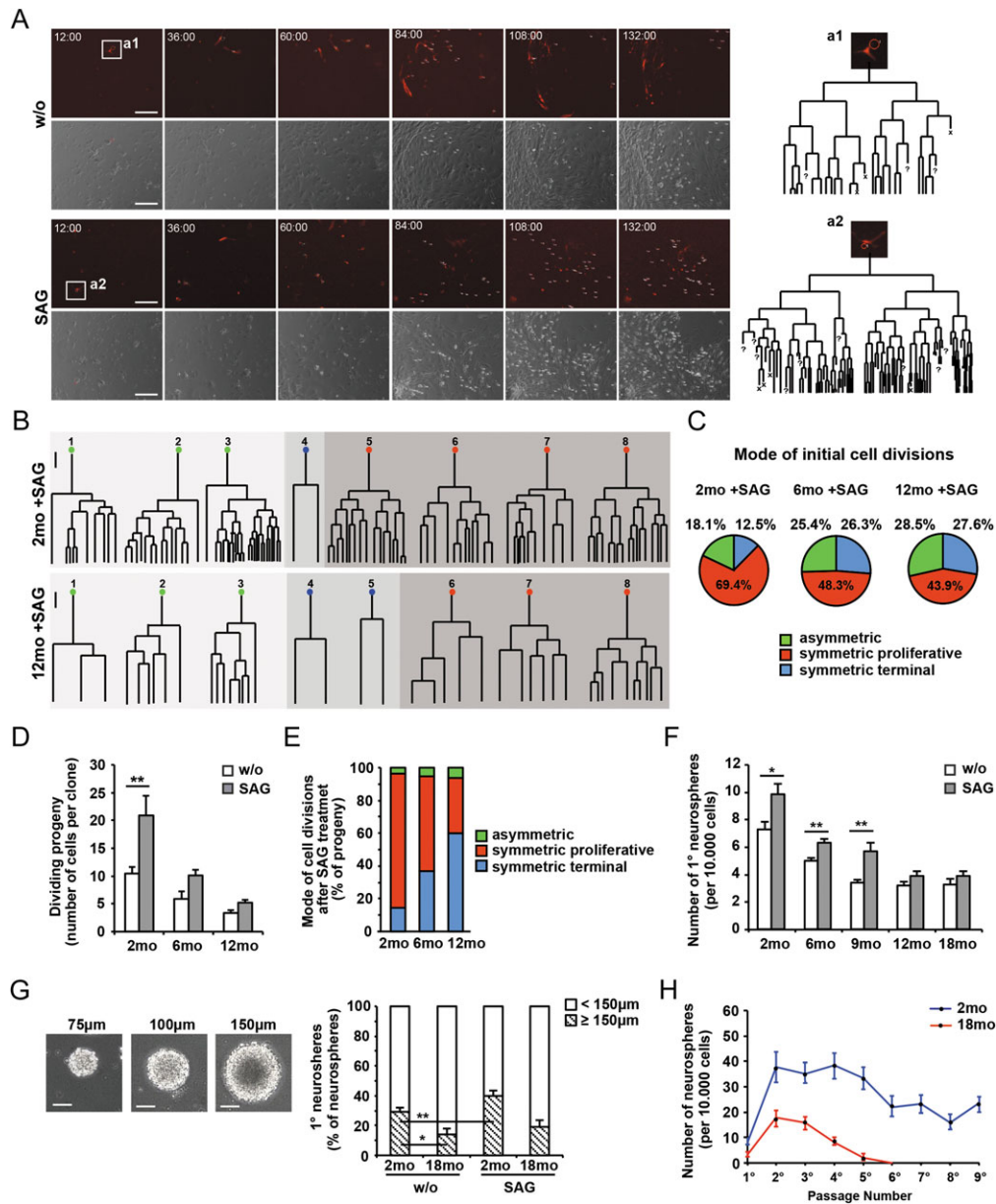


Figure 5. Modulation of Shh signaling induces re-entering in the cell cycle of young but not aged reactive astrocytes. (A) Time-lapse sequences obtained by video microscopy (RFP in upper panel, phase-contrast in lower panel) at different time points (hour:minute) show examples of cell colonies generated from single GFAP+/hGeminin+ cells under control condition (w/o, a1) or in SAG-containing culture medium (a2). Lineage trees show the effect of SAG addition, which in contrast to the control situation (a1), largely mediated generation of proliferating progeny from single GFAP-RFP+/mAG-hGeminin+ cell (a2) (“x” indicates cell death and cells that moved out the visual field are marked with “?”). (B) Overview of distinct lineage trees obtained from dividing GFAP+/hGeminin+ cells in the SAG-containing cultures isolated from 2- and 12-month-old animals at 5 dpi. (C) Pie charts showing the percentage of asymmetrically, symmetrically terminal, or proliferative dividing astrocytes obtained from 2-, 6-, and 12-month-old animals at 5 dpi and cultured in the presence of SAG for 7 day. (D) Bar charts depict the age-associated decrease in the number of dividing progeny among all daughter cells generated from single GFAP+/hGeminin+ cells in SAG-containing culture medium. (E) A progressive age-related exhaustion of symmetrically proliferating progeny mirrors the loss of self-renewal in reactive astrocytes, even after exposure to SAG. (F) Statistical analysis uncovered the significant age-dependent reduction of neurosphere-forming cells in the penumbra, with no significant changes by exposure to SAG in vitro. (G) Analyses of individual neurospheres at 14div revealed that the aged reactive astrocytes give rise to smaller neurospheres, even in the presence of SAG in the culture medium. (H) Quantification of neurosphere numbers per 10,000 plated cells indicated the reduced long-term capacity to self-renew of neurospheres derived from aged (red line) compared to young (blue line) reactive astrocytes. All data are plotted as mean \pm SEM from $n \geq 3$ experiments. Significance between means was analyzed using 2-tailed unpaired Student’s *t*-test or between multiple groups by 1-way ANOVA test and indicated as **P*-value < 0.05, ***P*-value < 0.01, and ****P*-value < 0.001. Scale bars: 40 μ m in (A) and 50 μ m in (G).

neurosphere formation. Of note, our stab wound injury paradigm is restricted to the GM and placed in the somatosensory cerebral cortex at a distance sufficient to avoid migration from the stem cell niche, the subependymal zone (SEZ) (Buffo et al. 2008; Sirko et al. 2013, 2015). At 5 dpi, cells from the GM

surrounding the injury site in animals of all age groups were dissociated and plated in neurosphere medium for 14 days. Notably, we observed that the number of neurosphere-forming cells decreased in an age-dependent manner, with less than half the number of neurospheres obtained from reactive glia

isolated from 18-month-old animals (Fig. 5F). While the number of neurospheres is an indicator for the number of cells with stem cell properties, the diameter of neurospheres reflects the proliferative activity of these cells and their progeny. As expected from the above analysis, young reactive astrocytes, in contrast to the old ones, generated a significantly higher number of large neurospheres ($\geq 150 \mu\text{m}$) (Fig. 5G), indicating that the age-related decline in NSC numbers is also paralleled with an age-related decline in proliferation kinetics within individual neurospheres. This reduced expansion of neurosphere cells is well consistent with a progressive failure of aging reactive astrocytes to divide repeatedly, as previously observed under adherent culture conditions. Moreover, passaging of primary neurospheres of equivalent size (100–150 μm in diameter) and, hence, approximately equivalent cell numbers, resulted in a significantly lower number of secondary neurospheres in cultures derived from old compared to young mice. This finding indicated an age-related decrease in the proportion of self-renewing NSCs within the neurospheres, consistent with increased symmetric terminal divisions of reactive astrocytes observed above by time-lapse imaging. Notably, the serial passaging of neurospheres at a constant cell density showed that neurospheres formed in cultures of cells from old mice displayed significantly reduced self-renewal capacity compared to cultures from young mice, with a complete exhaustion of neurosphere cultures derived from 18-month-old mice already after the passage 5. This reduced self-renewal of neurospheres thus demonstrates a severe restriction in the self-renewal capacity of the few cells with the NSC capacity observed after stab wound injury in 18-month-old mice (Fig. 5H).

As expected from the above experiments, SAG addition to the culture medium could no longer increase the number of primary neurospheres formed from reactive glia derived from 12- or 18-month-old mice, while a significant increase was detected for cells derived from younger animals (Fig. 5F). Besides the modulation of neurosphere-forming capacity, the presence of SAG also stimulated the proliferation of cells within neurospheres, as evident by the significantly higher number of larger primary neurospheres, especially in SAG-treated cultures from young animals (Fig. 5G). A tendency to form larger neurospheres was observed in cultures derived from the GM injury site of 18-month-old mice, nevertheless they were quite rare, generally less than 20% of all neurospheres (vs. ~40% in cultures of young GM cells) (Fig. 5G). Accordingly, addition of SAG could not significantly boost the neurosphere-forming capacity in aged reactive astrocytes, thus resulting in the appearance of fewer and smaller primary neurospheres.

Discussion

In this study, we investigated the impact of aging on the injury-induced plasticity in cerebrocortical astrocytes, and are now demonstrating that aged reactive astrocytes in the post-traumatic somatosensory GM display an altered proliferative phenotype that subsequently leads to reduction of astrocyte numbers in the injured GM parenchyma.

In light of the highly heterogeneous and region-specific effects of aging on astrocytes (Shapira et al. 2002; Toescu 2005; Lewis et al. 2012; Rodriguez-Arellano et al. 2016), we first demonstrated the changes in the somatosensory GM astrocytes in relation to physiological aging in mice. Our observations show that astrocytes in this area of the cerebral cortex acquire an activated state in the upper layers with aging, and similarly to astrocytes in other regions of brain (Rodriguez et al. 2014),

display upregulation of GFAP starting already in middle-aged animals. However, in contrast to astrocytes within, for example, the entorhinal cortex (Rodriguez et al. 2014), GFAP+ astrocytes in the somatosensory GM also develop a hypertrophic morphology. This switch of state in aging cortical astrocytes is paralleled with changes at the transcriptional level indicating “certain” alterations in astrocyte physiology with age. We found, for instance, that the GFAP+ astrocytes from the old somatosensory GM exhibit in average about ~30% higher levels of Glul mRNA (glutamine synthetase, GS) than GFAP+ astrocytes in this GM region of young brains (see Supplementary Fig. 1C). As a central enzyme for glutamine–glutamate/GABA shuttle and for ammonium detoxification, GS is an essential part of the astrocyte–neuron signaling process (Rose et al. 2013) and changes in GS expression and/or activity may lead to different brain pathologies, including neurodegenerative diseases and mental disorders (Steffens et al. 2005; Steffek et al. 2008; Sun et al. 2013). Interestingly, while an increased expression of GS through ischemic postconditioning has been shown to be neuroprotective in ischemic rats (Zhang et al. 2011), it appears that the region-selective alterations in GS expression during physiological aging (Rodriguez et al. 2014) are related to the changes along a metabolic–inflammatory axis that support the functionality switch of astrocytes from neurotrophic to neurotoxic with age (Rose and Felipo 2005; Jiang and Cadenas 2014). Indeed, there is a tight association between alterations in metabolic functions and an increased expression of genes characteristic for an inflammatory state because of astrocyte aging (Orre et al. 2014). Thus, acquisition of an inflammatory phenotype in astrocytes during physiological aging may be the cause/consequence of either local or systemic imbalance between pro- and anti-inflammatory cytokine levels occurring with age (von Bernhardt et al. 2015), thus favoring the so-called “inflammaging” theory, which regard brain aging as a chronic neuroinflammation (Franceschi 2007). However, our observations suggest considerable regional specificity in both the degree and cellular basis of the “inflammaging”. First, in contrast to other brain regions where microglia adopt an activated state during aging (von Bernhardt et al. 2010), we found no significant differences either in the number or morphology of microglia between the somatosensory GM of young and old mice. Second, although glia in several brain regions respond to aging with an increased proliferation (Buga et al. 2008; Acaz-Fonseca et al. 2015), we did not find any signs of induced proliferative activity either in astrocytes or in other types of glia in the somatosensory GM of middle-aged or even aged mice. These observations are also corroborated by genome-wide expression analysis showing a markedly upregulated expression of anti-proliferation genes (including cyclin-dependent kinase inhibitor 1B, also known as p27) in the healthy cerebral cortex of aged rats (Buga et al. 2008). In this context, our data also show that the total number of astrocytes in this cerebral region does not change, indicating maintenance of the astroglial population within their physiological range during aging.

Our observations in the intact GM thus provide support for the concept of regional specificity of age-related dysregulations in the signaling events (Raz et al. 2005; Rodriguez et al. 2014; von Bernhardt et al. 2015; Verkhratsky et al. 2016), which can also be translated into the region-specific response of aging glia, including the reaction of aged astrocytes to injury. As with prior studies of post-injured aged animals (Badan et al. 2003; Acaz-Fonseca et al. 2015; Chisholm et al. 2015; Moraga et al. 2015), the stab wounding to the somatosensory GM induces severe reactive gliosis in aged mice. Also in agreement with previous studies,

we found that the process of aging progressively increases the proliferative response in the post-traumatic GM (as shown by the numbers of BrdU+ cells), especially of microglia, since ~70% of BrdU+ cells in the aged group of animals corresponded to reactive Iba1+ microglia (see Supplementary Fig. 2A,B). Of particular importance, however, is the distinct response of other glial cells, the astrocytes, which show a continuous age-related decrease in proliferation in the post-traumatic GM. In fact, the frequency of proliferating astrocytes in aged mice was significantly reduced, compared with young mice. This observation is in agreement with previous reports demonstrating that astrocytes in aged post-stroke rats develop reduced proliferative response compared with young rats (Bugá et al. 2008; Acáz-Fonseca et al. 2015). However, in other areas of the brain, for example, the hippocampus, an age-related increase in astrocyte proliferation has been reported (Bugá et al. 2008; Acáz-Fonseca et al. 2015). The differences in the proliferative response of astrocytes suggest distinctive region-specific differences in astrocytes (Lundgaard et al. 2014), which might have a region-specific susceptibility to aging, reflecting distinct requirements for maintenance of their plasticity after injury.

In light of our finding that the injury-induced proliferative program fails to work in aging GM astrocytes, one of the main findings of our study is that this phenomenon is the consequence of changes in the multitude of their cell divisions. By our experimental approach *in vitro*, we provided the first demonstration that the proliferating reactive astrocytes progressively fail to re-enter the cell cycle with increasing age, while their cell-cycle length remains unaffected. This switch in the proliferative program adversely influences the outcome of astrocyte divisions, and sets the stage for a progressive depletion of the proliferating astrocyte pool over the course of aging along with a reduced stem cell potential. This raises the fundamental question of whether the loss of the potential to self-renew and proliferate in aging reactive astrocytes is entirely irreversible. Given that Shh not only controls the self-renewal rate of the astrocyte-like NSCs by modulation of their proliferative divisions in the adult SEZ (Ferent et al. 2014), but is also necessary and sufficient to promote stem cell properties in reactive astrocytes (Sirko et al. 2013), it was interesting to find that the treatment with SAG, which enhances the Shh pathway, mediates and increases proliferative divisions of reactive astrocytes from young but not aged animals. Consistent with this, the pool of proliferating astrocytes within the penumbra of aged GM still remains reduced following SAG-treatment *in vivo*.

It is important to note that the SAG-mediated activation of Smo induces the transcriptional activation of the Gli1 zinc finger transcription factors in young reactive astrocytes during the first 24 h after systemic SAG application (see Supplementary Fig. 3) indicating that SAG acts directly on the astrocytes. This is also corroborated by data showing that selective deletion of Smo in astrocytes using GLAST^{CreERT2}-mediated recombination or pharmacological inhibition of Smo significantly decreased transcriptional activation of the Shh/Gli signaling cascade and their effector Ccnd1 in reactive astrocytes, leading to the reduction in astrocyte proliferation and their stem cell response to the injury (Sirko et al. 2013). By these means, the age-related downregulation of Smo expression in astrocytes shown here may affect G1/S transition by the cell-cycle regulator Ccnd1, preventing thereby transition of aged reactive astrocytes from quiescent to cycling states, even after exposure to SAG. Nevertheless, there may be many other age-related alterations in other molecular pathways, such as Notch signaling. For example, the interaction between Shh and Notch signaling

pathways is required for the regulation of cell divisions during corticogenesis and in the adult SEZ (Ferent et al. 2014).

It was interesting to observe that the age-related reduction in the rate of reactive astrocyte proliferation is perpetuated also *in vitro*, where the complexity of the environment is reduced and no access to the lesion-derived diffusible morphogens from the liquor and serum at sites of disrupted blood-brain barrier (BBB) or other mediators produced by inflammatory cells at the injury site. Nonetheless, we cannot exclude that there are some modifications in the microenvironment of cultured cells due to the various factors secreted from microglia as they also exhibit phenotypic changes with age (Orre et al. 2014).

It is thus tempting to speculate that defects in the injury-induced plasticity of aged astrocytes is likely due to their intrinsic aging rather than due to reversible environmental changes, such as age-associated reduction of the Shh levels in plasma, niche, or systemically circulating factors (e.g., IGF-1, FGF-2, EGF, and VEGF) (El-Zaatari et al. 2012). The changes shown here further argue that the failure of astrocytes to elicit a proper proliferative response in the penumbra of aged brains likely reflects a manifestation of cell-intrinsic changes over the course of aging. Further work will have to address to what extent the age-dependent changes to the microenvironment may act either synergistically with intrinsic modifications or in addition to the decreased proliferation of reactive astrocytes. Our study characterized the changes to the proliferative program as a phenotypic characteristic of aged reactive astrocytes that provoke a decrease in the number of proliferating astrocytes in the aged post-traumatic GM. We further provided evidence suggesting the interference with Shh signaling pathway as implicated in the disability of aged astrocytes to renew themselves by either symmetric or asymmetric division. The challenge, therefore, will be to determine precisely these specific “off” mechanisms, which trigger the quiescent state of aged astrocytes throughout their response to injury of the cerebral cortex GM.

It should be noted that in analogy to reactive GM astrocytes, impairment of proliferation is also apparent in NSCs in the aged brain and linked to the depletion of their cell division, resulting in generation of nondividing progeny (Encinas et al. 2011; Lee et al. 2012; Calzolari et al. 2015). Several factors that underlie such an age-related limitation of NSC properties include the progressive lack of telomerase activity (Wong et al. 2003; Ferron et al. 2009; Jaskelioff et al. 2011). Interestingly, at this age the poststroke mice also show selectively affected proliferation of NSCs (also called Type-B cells) and Type-C cells, the proliferating progenitors that originate from the NSCs in the SEZ (Moraga et al. 2015). Since the proliferating GM astrocytes represent a plastic population of astroglia outside the neurogenic niches (Buffo et al. 2008; Sirko et al. 2009, 2013, 2015; Götz and Sirko 2013), the intrinsic changes to the proliferative/renewal program seem to be a common characteristic of proliferation-competent astroglia in the aged brain. It is, therefore, conceivable that mechanisms proposed to explain the intrinsic aging of NSCs, including telomere shortening, accumulation of DNA damage, or epigenetic alterations (Rando 2006; Drummond-Barbosa 2008) can also contribute to age-dependent exhaustion of proliferative activity in reactive GM astrocytes.

Since astrocyte proliferation is the only way to increase their numbers in the cortical GM (Bardehle et al. 2013), we have also demonstrated that insufficiency in maintaining proliferative astrocyte response in the aged post-injured GM ultimately results in the failure of astrocyte homeostasis in the penumbra

of aged mice. Given that restoration of the astroglial equilibrium represents an essential step to ensure certain repair mechanisms following tissue damage, that is, neuroprotection, proper reconstruction of the BBB, initiating and perpetuating cerebral immune response, physical fencing of the damaged areas or a removal of pathogens through phagocytosis (Cordiglieri and Farina 2010; Götz and Sirko 2013; Sirko et al. 2015; Verkhatsky et al. 2016), it is not surprising that an age-related deficit in the establishment of a particularly plastic and immature set of astrocytes (Fitch and Silver 2008) may in some instances alter the outcome after damage in the aged brain. Indeed, we have found that aged mice show an exacerbated parenchymal damage compared to younger animals at the same time point after injury, including a larger reactive perimeter within the penumbra as well as a higher number of infiltrating CD45+ cells in the injured GM parenchyma (data not shown). Moreover, it is also conceivable that the significantly prolonged BBB leakage in the post-traumatic GM of old animals (Supplementary Fig. 4) can influence survival rate of astrocytes at the injury site, and in addition to the drop of proliferating astrocytes, can contribute to a loss of astrocytes in the parenchyma surrounding the lesion in the aged brain. In addition, premature formation of scar-like tissue as well as diminished poststroke recovery of aged animals have been previously correlated also with abnormal reactivity of aging glial cells to damage in the brain (Acaz-Fonseca et al. 2015; Moraga et al. 2015).

Thus, our present results not only extend previous findings on age-related effects of the response of glial cells to an invasive injury but also highlight that cell-intrinsic changes in reactive astrocytes contribute to the adverse outcome of astrocyte proliferation within the injured GM parenchyma, affecting thereby astrocyte homeostasis in the damaged area. Future studies should, therefore, focus on a region-specific analysis of reactive astrocyte plasticity during aging, since our present data support the hypothesis that the decline in regenerative potential and impairment of post-traumatic recovery of brain parenchyma during aging may result from specific age-related changes in astrocyte proliferation.

Supplementary Material

Supplementary material is available at *Cerebral Cortex* online.

Funding

This work was supported by the Friedrich Baur Foundation (Grant nos. 822646 and 822395 to S.S.); the German Research Foundation (SPP 1757 and SFB 870 to M.G.); the European Research Council (Grant no. 340793 to M.G.); Excellence Cluster of Systems Neurology Synergy (M.G.) and the Helmholtz Alliance Icomed (M.G.).

Notes

We thank Tatiana Simon-Ebert and Detlef Franzen for great technical assistance, and Dr. Stefan H. Stricker for excellent comments on the manuscript. *Conflict of Interest*: None declared.

References

- Acaz-Fonseca E, Duran JC, Carrero P, Garcia-Segura LM, Arevalo MA. 2015. Sex differences in glia reactivity after cortical brain injury. *Glia*. 63:1966–1981.
- Alexander MP. 1994. Stroke rehabilitation outcome. A potential use of predictive variables to establish levels of care. *Stroke*. 25:128–134.
- Anderson MA, Burda JE, Ren Y, Ao Y, O'Shea TM, Kawaguchi R, Coppola G, Khakh BS, Deming TJ, Sofroniew MV. 2016. Astrocyte scar formation aids central nervous system axon regeneration. *Nature*. 532:195–200.
- Badan I, Buchhold B, Hamm A, Gratz M, Walker LC, Platt D, Kessler C, Popa-Wagner A. 2003. Accelerated glial reactivity to stroke in aged rats correlates with reduced functional recovery. *J Cereb Blood Flow Metab*. 23:845–854.
- Bambakidis NC, Petrullis M, Kui X, Rothstein B, Karampelas I, Kuang Y, Selman WR, LaManna JC, Miller RH. 2012. Improvement of neurological recovery and stimulation of neural progenitor cell proliferation by intrathecal administration of Sonic hedgehog. *J Neurosurg*. 116:1114–1120.
- Bardehle S, Kruger M, Buggenthin F, Schwausch J, Ninkovic J, Clevers H, Snippert HJ, Theis FJ, Meyer-Luehmann M, Bechmann I, et al. 2013. Live imaging of astrocyte responses to acute injury reveals selective juxtavascular proliferation. *Nat Neurosci*. 16:580–586.
- Buffo A, Rite I, Tripathi P, Lepier A, Colak D, Horn AP, Mori T, Gotz M. 2008. Origin and progeny of reactive gliosis: a source of multipotent cells in the injured brain. *Proc Natl Acad Sci USA*. 105:3581–3586.
- Buga AM, Sascau M, Pisoschi C, Herndon JG, Kessler C, Popa-Wagner A. 2008. The genomic response of the ipsilateral and contralateral cortex to stroke in aged rats. *J Cell Mol Med*. 12:2731–2753.
- Burda JE, Sofroniew MV. 2014. Reactive gliosis and the multicellular response to CNS damage and disease. *Neuron*. 81:229–248.
- Calzolari F, Michel J, Baumgart EV, Theis F, Gotz M, Ninkovic J. 2015. Fast clonal expansion and limited neural stem cell self-renewal in the adult subependymal zone. *Nat Neurosci*. 18:490–492.
- Chisholm NC, Henderson ML, Selvamani A, Park MJ, Dindot S, Miranda RC, Sohrabji F. 2015. Histone methylation patterns in astrocytes are influenced by age following ischemia. *Epigenetics*. 10:142–152.
- Copen WA, Schwamm LH, Gonzalez RG, Wu O, Harmath CB, Schaefer PW, Koroshetz WJ, Sorensen AG. 2001. Ischemic stroke: effects of etiology and patient age on the time course of the core apparent diffusion coefficient. *Radiology*. 221:27–34.
- Cordiglieri C, Farina C. 2010. Astrocytes exert and control immune responses in the brain. *Curr Immunol Rev*. 6:150–159.
- Costa MR, Ortega F, Brill MS, Beckervordersandforth R, Petrone C, Schroeder T, Gotz M, Berninger B. 2011. Continuous live imaging of adult neural stem cell division and lineage progression in vitro. *Development*. 138:1057–1068.
- Dostovic Z, Smajlovic D, Sinanovic O, Vidovic M. 2009. Duration of delirium in the acute stage of stroke. *Acta Clin Croat*. 48:13–17.
- Drummond-Barbosa D. 2008. Stem cells, their niches and the systemic environment: an aging network. *Genetics*. 180:1787–1797.
- El-Zaatari M, Daignault S, Tessier A, Kelsey G, Travnikar LA, Cantu EF, Lee J, Plonka CM, Simeone DM, Anderson MA, et al. 2012. Plasma Shh levels reduced in pancreatic cancer patients. *Pancreas*. 41:1019–1028.
- Encinas JM, Michurina TV, Peunova N, Park JH, Tordo J, Peterson DA, Fishell G, Koulakov A, Enikolopov G. 2011.

- Division-coupled astrocytic differentiation and age-related depletion of neural stem cells in the adult hippocampus. *Cell Stem Cell*. 8:566–579.
- Ferent J, Cochard L, Faure H, Taddei M, Hahn H, Ruat M, Traiffort E. 2014. Genetic activation of Hedgehog signaling unbalances the rate of neural stem cell renewal by increasing symmetric divisions. *Stem Cell Rep*. 3:312–323.
- Ferron SR, Marques-Torres MA, Mira H, Flores I, Taylor K, Blasco MA, Farinas I. 2009. Telomere shortening in neural stem cells disrupts neuronal differentiation and neurogenesis. *J Neurosci*. 29:14394–14407.
- Fitch MT, Silver J. 2008. CNS injury, glial scars, and inflammation: Inhibitory extracellular matrices and regeneration failure. *Exp Neurol*. 209:294–301.
- Fonarow GC, Reeves MJ, Zhao X, Olson DM, Smith EE, Saver JL, Schwamm LH, Get With the Guidelines-Stroke Steering C, Investigators. 2010. Age-related differences in characteristics, performance measures, treatment trends, and outcomes in patients with ischemic stroke. *Circulation*. 121:879–891.
- Franceschi C. 2007. Inflammaging as a major characteristic of old people: can it be prevented or cured? *Nutr Rev*. 65: S173–S176.
- Frank-Kamenetsky M, Zhang XM, Bottega S, Guicherit O, Wichterle H, Dudek H, Bumcrot D, Wang FY, Jones S, Shulok J, et al. 2002. Small-molecule modulators of Hedgehog signaling: identification and characterization of smoothed agonists and antagonists. *J Biol*. 1:10.
- Galvan V, Jin K. 2007. Neurogenesis in the aging brain. *Clin Interv Aging*. 2:605–610.
- Gargano JW, Wehner S, Reeves MJ. 2011. Presenting symptoms and onset-to-arrival time in patients with acute stroke and transient ischemic attack. *J Stroke Cerebrovasc Dis*. 20:494–502.
- Götz M, Sirko S. 2013. Potential of glial cells. In: Sell S, editor. *Stem cells handbook*. 2nd ed. New York: Springer. p. 347–361.
- Heinrich C, Bergami M, Gascon S, Lepier A, Vigano F, Dimou L, Sutor B, Berninger B, Gotz M. 2014. Sox2-mediated conversion of NG2 glia into induced neurons in the injured adult cerebral cortex. *Stem Cell Reports*. 3:1000–1014.
- Heintz N. 2004. Gene expression nervous system atlas (GENSAT). *Nat Neurosci*. 7:483.
- Herrmann JE, Imura T, Song B, Qi J, Ao Y, Nguyen TK, Korsak RA, Takeda K, Akira S, Sofroniew MV. 2008. STAT3 is a critical regulator of astrogliosis and scar formation after spinal cord injury. *J Neurosci*. 28:7231–7243.
- Hilsenbeck O, Schwarzfischer M, Skylaki S, Schaubberger B, Hoppe PS, Loeffler D, Kokkalis KD, Hastreiter S, Skylaki E, Filipczyk A, et al. 2016. Software tools for single-cell tracking and quantification of cellular and molecular properties. *Nat Biotechnol*. 34:703–706.
- Hirrlinger PG, Scheller A, Braun C, Quintela-Schneider M, Fuss B, Hirrlinger J, Kirchhoff F. 2005. Expression of reef coral fluorescent proteins in the central nervous system of transgenic mice. *Mol Cell Neurosci*. 30:291–303.
- Jaskeliouff M, Muller FL, Paik JH, Thomas E, Jiang S, Adams AC, Sahin E, Kost-Alimova M, Protopopov A, Cadinanos J, et al. 2011. Telomerase reactivation reverses tissue degeneration in aged telomerase-deficient mice. *Nature*. 469:102–106.
- Jiang T, Cadenas E. 2014. Astrocytic metabolic and inflammatory changes as a function of age. *Aging Cell*. 13:1059–1067.
- Juraska JM, Lowry NC. 2012. Neuroanatomical changes associated with cognitive aging. *Curr Top Behav Neurosci*. 10:137–162.
- Lee SW, Clemenson GD, Gage FH. 2012. New neurons in an aged brain. *Behav Brain Res*. 227:497–507.
- Levine J, Kwon E, Paez P, Yan W, Czerwiec G, Loo JA, Sofroniew MV, Wanner IB. 2016. Traumatically injured astrocytes release a proteomic signature modulated by STAT3-dependent cell survival. *Glia*. 64:668–694.
- Lewis DK, Thomas KT, Selvamani A, Sohrabji F. 2012. Age-related severity of focal ischemia in female rats is associated with impaired astrocyte function. *Neurobiol Aging*. 33:1123 e1121–1116.
- Livak KJ, Schmittgen TD. 2001. Analysis of relative gene expression data using real-time quantitative PCR and the 2(-Delta Delta C(T)) Method. *Methods*. 25:402–408.
- Lundgaard I, Osorio MJ, Kress BT, Sanggaard S, Nedergaard M. 2014. White matter astrocytes in health and disease. *Neuroscience*. 276:161–173.
- Lynch AM, Murphy KJ, Deighan BF, O'Reilly JA, Gun'ko YK, Cowley TR, Gonzalez-Reyes RE, Lynch MA. 2010. The impact of glial activation in the aging brain. *Aging Dis*. 1:262–278.
- Middeldorp J, Hol EM. 2011. GFAP in health and disease. *Prog Neurobiol*. 93:421–443.
- Moppett IK. 2007. Traumatic brain injury: assessment, resuscitation and early management. *Br J Anaesth*. 99:18–31.
- Moraga A, Pradillo JM, Garcia-Culebras A, Palma-Tortosa S, Ballesteros I, Hernandez-Jimenez M, Moro MA, Lizasoain I. 2015. Aging increases microglial proliferation, delays cell migration, and decreases cortical neurogenesis after focal cerebral ischemia. *J Neuroinflammation*. 12:87.
- Nolte C, Matyash M, Pivneva T, Schipke CG, Ohlemeyer C, Hanisch UK, Kirchhoff F, Kettenmann H. 2001. GFAP promoter-controlled EGFP-expressing transgenic mice: a tool to visualize astrocytes and astrogliosis in living brain tissue. *Glia*. 33:72–86.
- O'Callaghan JP, Kelly KA, VanGilder RL, Sofroniew MV, Miller DB. 2014. Early activation of STAT3 regulates reactive astrogliosis induced by diverse forms of neurotoxicity. *PLoS ONE*. 9:e102003.
- Orre M, Kamphuis W, Osborn LM, Melief J, Koopman L, Huitinga I, Klooster J, Bossers K, Hol EM. 2014. Acute isolation and transcriptome characterization of cortical astrocytes and microglia from young and aged mice. *Neurobiol Aging*. 35:1–14.
- Ortega F, Berninger B, Costa MR. 2013. Primary culture and live imaging of adult neural stem cells and their progeny. *Methods Mol Biol*. 1052:1–11.
- Pekna M, Pekny M, Nilsson M. 2012. Modulation of neural plasticity as a basis for stroke rehabilitation. *Stroke*. 43:2819–2828.
- Rando TA. 2006. Stem cells, ageing and the quest for immortality. *Nature*. 441:1080–1086.
- Raz N, Lindenberger U, Rodrigue KM, Kennedy KM, Head D, Williamson A, Dahle C, Gerstorf D, Acker JD. 2005. Regional brain changes in aging healthy adults: general trends, individual differences and modifiers. *Cereb Cortex*. 15:1676–1689.
- Rieger MA, Hoppe PS, Smejkal BM, Eitelhuber AC, Schroeder T. 2009. Hematopoietic cytokines can instruct lineage choice. *Science*. 325:217–218.
- Rodriguez JJ, Yeh CY, Terzieva S, Olabarria M, Kulijewicz-Nawrot M, Verkhatsky A. 2014. Complex and region-specific changes in astroglial markers in the aging brain. *Neurobiol Aging*. 35:15–23.
- Rodriguez-Arellano JJ, Parpura V, Zorec R, Verkhatsky A. 2016. Astrocytes in physiological aging and Alzheimer's disease. *Neuroscience*. 323:170–182.

- Rose C, Felipo V. 2005. Limited capacity for ammonia removal by brain in chronic liver failure: potential role of nitric oxide. *Metab Brain Dis.* 20:275–283.
- Rose CF, Verkhratsky A, Parpura V. 2013. Astrocyte glutamine synthetase: pivotal in health and disease. *Biochem Soc Trans.* 41:1518–1524.
- Sakaue-Sawano A, Kurokawa H, Morimura T, Hanyu A, Hama H, Osawa H, Kashiwagi S, Fukami K, Miyata T, Miyoshi H, et al. 2008. Visualizing spatiotemporal dynamics of multicellular cell-cycle progression. *Cell.* 132:487–498.
- Shapira S, Sapir M, Wengier A, Grauer E, Kadar T. 2002. Aging has a complex effect on a rat model of ischemic stroke. *Brain Res.* 925:148–158.
- Simon C, Gotz M, Dimou L. 2011. Progenitors in the adult cerebral cortex: cell cycle properties and regulation by physiological stimuli and injury. *Glia.* 59:869–881.
- Sirko S, Neitz A, Mittmann T, Horvat-Brocker A, von Holst A, Eysel UT, Faissner A. 2009. Focal laser-lesions activate an endogenous population of neural stem/progenitor cells in the adult visual cortex. *Brain.* 132:2252–2264.
- Sirko S, Behrendt G, Johansson PA, Tripathi P, Costa M, Bek S, Heinrich C, Tiedt S, Colak D, Dichgans M, et al. 2013. Reactive glia in the injured brain acquire stem cell properties in response to sonic hedgehog. [corrected]. *Cell Stem Cell.* 12:426–439.
- Sirko S, Irmeler M, Gascon S, Bek S, Schneider S, Dimou L, Obermann J, De Souza Paiva D, Poirier F, Beckers J, et al. 2015. Astrocyte reactivity after brain injury: The role of galectins 1 and 3. *Glia.* 63:2340–2361.
- Sofroniew MV. 2009. Molecular dissection of reactive astrogliosis and glial scar formation. *Trends Neurosci.* 32:638–647.
- Sriram K, Benkovic SA, Hebert MA, Miller DB, O'Callaghan JP. 2004. Induction of gp130-related cytokines and activation of JAK2/STAT3 pathway in astrocytes precedes up-regulation of glial fibrillary acidic protein in the 1-methyl-4-phenyl-1,2,3,6-tetrahydropyridine model of neurodegeneration: key signaling pathway for astrogliosis in vivo? *J Biol Chem.* 279:19936–19947.
- Steffek AE, McCullumsmith RE, Haroutunian V, Meador-Woodruff JH. 2008. Cortical expression of glial fibrillary acidic protein and glutamine synthetase is decreased in schizophrenia. *Schizophr Res.* 103:71–82.
- Steffens M, Huppertz HJ, Zentner J, Chauzit E, Feuerstein TJ. 2005. Unchanged glutamine synthetase activity and increased NMDA receptor density in epileptic human neocortex: implications for the pathophysiology of epilepsy. *Neurochem Int.* 47:379–384.
- Sun HL, Zhang SH, Zhong K, Xu ZH, Feng B, Yu J, Fang Q, Wang S, Wu DC, Zhang JM, et al. 2013. A transient upregulation of glutamine synthetase in the dentate gyrus is involved in epileptogenesis induced by amygdala kindling in the Rat. *PLoS ONE.* 8:e66885.
- Toescu EC. 2005. Normal brain ageing: models and mechanisms. *Philos Trans R Soc Lond B Biol Sci.* 360:2347–2354.
- Unger JW. 1998. Glial reaction in aging and Alzheimer's disease. *Microsc Res Tech.* 43:24–28.
- Verkhratsky A, Parpura V, Pekna M, Pekny M, Sofroniew M. 2014a. Glia in the pathogenesis of neurodegenerative diseases. *Biochem Soc Trans.* 42:1291–1301.
- Verkhratsky A, Rodriguez JJ, Parpura V. 2014b. Neuroglia in ageing and disease. *Cell Tissue Res.* 357:493–503.
- Verkhratsky A, Zorec R, Rodriguez JJ, Parpura V. 2016. Astroglial dynamics in ageing and Alzheimer's disease. *Curr Opin Pharmacol.* 26:74–79.
- von Bernhardi R, Tichauer JE, Eugenin J. 2010. Aging-dependent changes of microglial cells and their relevance for neurodegenerative disorders. *J Neurochem.* 112:1099–1114.
- von Bernhardi R, Eugenin-von Bernhardi L, Eugenin J. 2015. Microglial cell dysregulation in brain aging and neurodegeneration. *Front Aging Neurosci.* 7:124.
- Wong KK, Maser RS, Bachoo RM, Menon J, Carrasco DR, Gu Y, Alt FW, DePinho RA. 2003. Telomere dysfunction and Atm deficiency compromises organ homeostasis and accelerates ageing. *Nature.* 421:643–648.
- Yun HM, Kim JA, Hwang CJ, Jin P, Baek MK, Lee JM, Hong JE, Lee SM, Han SB, Oh KW, et al. 2015. Neuroinflammatory and amyloidogenic activities of IL-32beta in Alzheimer's disease. *Mol Neurobiol.* 52:341–352.
- Zamanian JL, Xu L, Foo LC, Nouri N, Zhou L, Giffard RG, Barres BA. 2012. Genomic analysis of reactive astrogliosis. *J Neurosci.* 32:6391–6410.
- Zhang L, Zhang RL, Wang Y, Zhang C, Zhang ZG, Meng H, Chopp M. 2005. Functional recovery in aged and young rats after embolic stroke: treatment with a phosphodiesterase type 5 inhibitor. *Stroke.* 36:847–852.
- Zhang W, Miao Y, Zhou S, Jiang J, Luo Q, Qiu Y. 2011. Neuroprotective effects of ischemic postconditioning on global brain ischemia in rats through upregulation of hippocampal glutamine synthetase. *J Clin Neurosci.* 18:685–689.